

Effects of magnetic dipolar interactions on the specific time constant in superparamagnetic nanoparticle systems

This content has been downloaded from IOPscience. Please scroll down to see the full text.

2016 J. Phys. D: Appl. Phys. 49 295001

(<http://iopscience.iop.org/0022-3727/49/29/295001>)

View [the table of contents for this issue](#), or go to the [journal homepage](#) for more

Download details:

IP Address: 142.66.3.42

This content was downloaded on 05/07/2016 at 08:27

Please note that [terms and conditions apply](#).

Effects of magnetic dipolar interactions on the specific time constant in superparamagnetic nanoparticle systems

N Iacob^{1,4}, G Schinteie², C Bartha², P Palade², L Vekas³ and V Kuncser²

¹ National Institute for Lasers, Plasma and Radiation Physics, PO Box MG-36, 077125 Bucharest-Magurele, Romania

² National Institute of Materials Physics, PO Box MG-7, 077125 Bucharest-Magurele, Romania

³ Laboratory of Magnetic Fluids, Centre for Fundamental and Advanced Technical Research, Romanian Academy-Timisoara Division, Timisoara 300223, Romania

⁴ Faculty of Physics, University of Bucharest, Bucharest-Magurele 077125, Romania

E-mail: kuncser@infim.ro

Received 25 February 2016, revised 25 May 2016

Accepted for publication 26 May 2016

Published 29 June 2016



Abstract

A quantitative treatment of the effects of magnetic mutual interactions on the specific absorption rate of a superparamagnetic system of iron oxide nanoparticles coated with oleic acid is reported. The nanoparticle concentration of the considered ferrofluid samples varied from a very low (0.005) to a medium (0.16) value of the volume fraction, whereas the amplitude of the exciting AC magnetic field ranged from 14–35 kA m⁻¹. It was proved that a direct effect of the interparticle interactions resides in the regime of the modified superparamagnetism, dealing, besides the usual increase in the anisotropy energy barrier per nanoparticle, with the decrease in the specific time constant τ_0 of the relaxation law, usually considered as a material constant. Consequently, the increase in the specific absorption rate versus the volume fraction is significantly diminished in the presence of the interparticle interactions compared to the case of non-interacting superparamagnetic nanoparticles, with direct influence on the magnetic hyperthermia efficiency.

Keywords: modified superparamagnetism, relaxation time constant, dipolar interactions, magnetic relaxation, specific absorption rate

(Some figures may appear in colour only in the online journal)

1. Introduction

Besides various nanotechnology related applications of superparamagnetic nanoparticles (NPs) such as magnetic data storage [1], magnetic sensors [2], etc, there are also interesting biomedical applications as, for example, magnetic resonance imaging [3], drug targeting [4, 5], cancer therapy [6–8], etc. While most of these applications are related to the superparamagnetic relaxation phenomena, there was a particular focus on the investigation of the magnetic inter-particle interactions regarding their superparamagnetic behavior [9–11]. The nature of the interactions that may occur in a nanoparticle system is influenced by the mutual distance between particles (depending on their concentration). If the NPs are in close

contact, exchange interactions (direct or super-exchange) may appear between magnetic atoms at the NP surface [12, 13]. Ruderman–Kittel–Kasuya–Yosida (RKKY) is another type of interaction (mediated by the conduction electrons) which can appear for NPs dispersed in a metallic matrix [14]. Tunneling exchange interaction can be present among NPs dispersed in a non-metallic matrix, if the inter-particle distances decrease to the sub-nanometer scale [15]. Except for the already-mentioned interactions, which are usually of the short-range type and involve peculiar conditions, long-range dipolar interactions act among the giant magnetic moments associated to each magnetic NP [16]. These interactions play a crucial role in contactless nanoparticulate systems and depend strongly on the particle concentration. According to the Stoner–Wolffarth

model, in a single-domain magnetic nanoparticle with uniaxial anisotropy, the magnetic moment of the nanoparticle fluctuates with respect to the easy axis (between the two energy minima) if the thermal energy ($k_B T$) overcomes the anisotropy energy barrier ($\Delta E = KV$). The characteristic time of this magnetic relaxation is given by the Neel–Brown formulation [17, 18]:

$$\tau = \tau_0 \exp(KV/k_B T) \quad (1)$$

where K is the anisotropy constant, V is the nanoparticle volume, T is the absolute temperature, k_B is the Boltzmann constant. τ_0 is a time constant specific to each material, taking values in a wide range (10^{-8} – 10^{-12} s). It is worth mentioning that there are different models for expressing the relaxation time (e.g. as reviewed by Dormann *et al* [19], all of them leading to a general form of type (1), but with different expressions for the time constant τ_0 . According to the reported relations for τ_0 [10, 19], this very slightly depends on the temperature, but depends on other material characteristics such as saturation magnetization, anisotropy constant, damping factor, gyromagnetic ratio, etc. Hence, the parameter τ_0 is considered to be a constant, specific to the material from which the superparamagnetic nanoparticles are synthesized.

In the peculiar case of a ferrofluid (magnetic NPs dispersed in a liquid phase) with a low-volume fraction, ϕ , of 10^{-3} (ϕ is the ratio between the volume of the magnetic solid fraction and the volume of the ferrofluid) and very narrow size distribution, the NP system forms a statistical assembly of identical and non-interacting magnetic entities (the relaxation behavior of the assembly can be described via the magnetic relaxation of a single particle). Increasing the particle concentration, the magnetic mutual interactions may either increase the characteristic relaxation time associated to an individual particle or even induce a new collective magnetic behavior of the system. Detailed reviews about different states generated by magnetic interactions among NPs, from modified superparamagnetism (SPM) to the collective state of superferromagnetism (SFM) or superspin glass (SSG) can be found in [20, 21]. In the general case of ferrofluids based on very fine particles which, in addition, are surfactant or functionalized, as required for bio-medical applications [22], the dipolar interactions can be supposed weak enough in order to lead to superspin collective states. Accordingly, the superparamagnetic relaxation process described by equation (1) could suffer just the following changes (as also mentioned in [21]):

- (i) The increase in the anisotropy energy barrier, leading to a modified SPM state described by relation (2):

$$\tau = \tau_0 \exp(\Delta E^*/k_B T). \quad (2)$$

- (ii) The manifestation of a ‘glass-like’ collective behavior at very low temperature that is quantitatively expressed by the insertion of a virtual transition temperature (T_0) in the denominator of relation (2) to separate the frozen magnetic state of quasi-independent macrospins from the randomly oriented interacting macrospins, as described by relation (3)

$$\tau = \tau_0 \exp(\Delta E^*/k_B(T - T_0)). \quad (3)$$

It is worth noting that in the case of dipolar interactions, each NP ‘sees’ a magnetic mean field, H_{ij} [19]:

$$H_{ij} = (M_j V_j / d_{ij}^3) [3(u_j \cdot r_{ij})r_{ij} - u_j] \quad (4)$$

where the product between the magnetization and the volume of a nanoparticle ($M_j V_j$) gives the overall magnetic moment associated to the nanoparticle, $u_{i,j}$ and r_{ij} are the unit vectors of the magnetic moments and of the distance (d_{ij}) between the centers of the i, j nanoparticles, respectively. According to [19], the expression for H_{ij} is depending on the shape of the nanoparticles and on their mutual distances. However, the dipolar interaction energy between two NPs is proportional to the product of their magnetic moments and inversely proportional to $(d_{ij})^3$.

The usual case of an increased anisotropy energy (and hence an increased blocking temperature, T_B , and an increased relaxation time τ under the assumption of an unmodified relaxation time constant, (τ_0) due to the interparticle interactions was modeled by Dormann *et al* [19]. On the other hand, Morup *et al* have reported, particularly through the evolution of the blocking temperature provided by Mossbauer spectroscopy, a decrease in the relaxation time at an increasing volume fraction of maghemite-based ferrofluid samples [23], proposing also a theoretical modeling of such behavior. In fact, Morup and Hansen [24] have also provided a critical review of different models dealing with the dynamics of interacting magnetic nanoparticles, concluding that both models by Dormann and, respectively, Morup are able to fit the experimental data, even if they are antagonistic. However, the models have to be applied according to independent estimations of the main parameters entering the expressions of the relaxation time (for example, the evolution of the anisotropy energy and the relaxation time constant). The different behavior of the energy barrier as a function of the interaction could be explained in Morup’s model via the temperature evolution of the multiplication factor $(1 - 3kT/4KV)$, which can shift from negative to positive values depending on the ratio between the thermal and anisotropy energies. In this context, the effect of the interparticle interactions on the relaxation time still remains an open issue, requiring both additional experimental and theoretical (including the most comprehensive micromagnetic simulations) considerations.

In biomedical applications, including cancer therapy via magnetic fluid hyperthermia (MFH) [25], magnetic nanoparticles are usually functionalized by covering them with a polymer layer [26, 27], which has the role of cutting the physical contact between the particles. Even under these special conditions, dipolar interactions are not vanishing for nanoparticle concentrations that are not too low. However, in this kind of application (MFH), small concentrations of magnetic nanoparticles are usually employed [28] in conjunction with the application of an AC magnetic field [29]. By magnetic relaxation processes [30], nanoparticles will dissipate enough heat to induce the death of the malignant cells. In spite of their functionalization, nanoparticles may accumulate (clusterize) locally in the intra- or extra-cellular medium of the target tumor [31]. Expectedly,

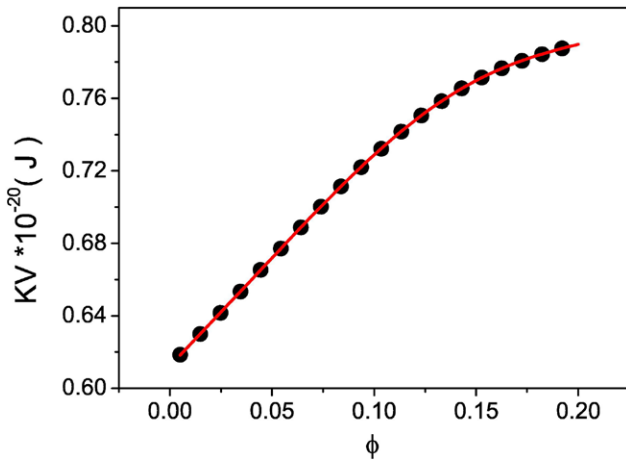


Figure 1. Effective anisotropy energy barrier KV versus volume fractions of ferrofluid samples.

the magnetic hyperthermia performances of nanoclusters and single nanoparticles could be quite different [32]. The aggregation processes lead to weaker or stronger dipolar interactions (depending on the local volume fraction) affecting the response of individual nanoparticles to the AC magnetic excitation. A range of spread effects of the interparticle interactions on the specific absorption rate (SAR) of particle systems has been reported to date [33–37]. Intrinsic magnetic features of NPs (anisotropy, magnetization) and experimental conditions (concentration, magnetic field) influence the heat dissipation pattern and may lead to diverging results [38].

Based on calorimetric measurements and using a previously developed methodology for the compensation of the heat losses [39], this paper investigates the possibility of getting valuable information on magnetic relaxation phenomena related to ferrofluid samples of different volume fractions by fitting the adiabatic heating curves with those simulated through a theoretical model [30] and taking into account the magnetic parameters of the nanoparticles as collected by magnetometry and Mössbauer measurements [40]. It is worth noting that in most of the ferrofluids of the high-volume fraction there is an agglomeration process of the nanoparticles leading to the formation of clusters of different sizes. However, the NPs inside the clusters are also interacting by weak dipolar interactions (antiferromagnetic in nature) due to the presence of a single/double layer of surfactant on each particle. As a result, the magnetic moment of the cluster is very small, whereas the relaxation mechanism of the NPs inside the cluster can be considered as a modified SPM one. The calorimetric measurements provide information on the average magnetic response, being dependent in a first approximation on the average volume fraction and not on its volumetric distribution (related to the cluster formation).

2. Experiment

The experimental setup, in the present work, uses a commercial RF heating system (Ambrell Easy Heating) of 4 kW power and equipped with a 235 kHz inductor coil built from eight turns of square section (4 mm^2) copper pipe cooled with

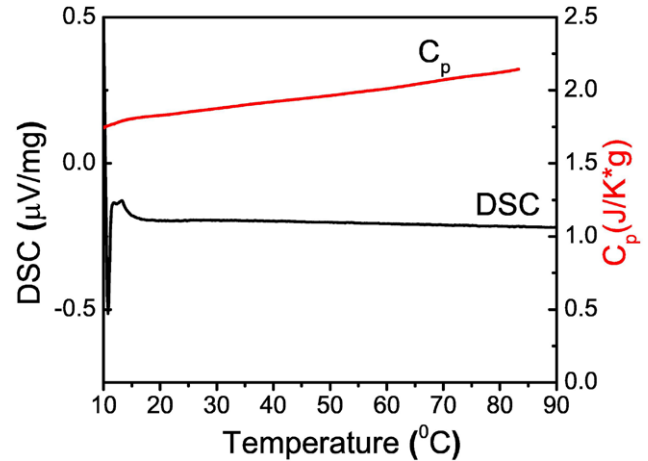


Figure 2. DSC typical measurement for the lowest diluted sample (black line) and temperature dependence of heat capacity (red line).

water. The coil has an inner diameter of 26 mm with a 2 mm distance between turns, which allows for the generation of a homogeneous magnetic field inside. Using this arrangement, described in detail in our previous works [39, 41], four ferrofluid samples of different volume fractions ($\phi_{1,2,3,4} = 0.005\text{--}0.16$) have been magnetically excited at four field intensities ($H_{0,1,2,3,4} = 14\text{--}35 \text{ kA m}^{-1}$). The temperature evolution of each sample was recorded from the thermal equilibrium (established between $20 \text{ }^\circ\text{C}$ – $30 \text{ }^\circ\text{C}$) to an optimal value depending on the field intensity (less than $70 \text{ }^\circ\text{C}$), by using an optical fiber thermometer connected to a computer. The ferrofluid samples, prepared via a chemical route [42], are based on iron oxide superparamagnetic nanoparticles (SPION) dispersed in transformer oil. The nanoparticles are coated with oleic acid, which has the role of preventing the physical contact between the magnetic core of the particles as well as the magnetic agglomeration, i.e. to ensure the long-term colloidal stability of the samples. Therefore, it can be stated that even at the maximum used concentration neither SSG nor SFM collective states could be involved. According to the morpho-structural and magnetic characterization presented previously [40], these particles have an ellipsoidal shape (with polar and equatorial diameters of 11.5 and 8.5 nm, respectively), and an average crystallite volume of about $4.3 \times 10^{-25} \text{ m}^3$. The saturation magnetization of the solid fraction (domain magnetization) was extracted from DC magnetometry measurements ($M_D = 4.5 \times 10^5 \text{ A m}^{-2}$). Also, the magnetic field inside the RF coil was numerically evaluated by the finite element method [41] for all inductor current intensities used in the experiment. The effective anisotropy energy barrier KV of each ferrofluid sample was extrapolated (figure 1) from the existing data provided by Mössbauer spectroscopy [40]. It is worth mentioning that the correspondence between the volume fraction and the KV values for similar samples of different volume fractions was shown to be in agreement with the presence of increasing dipolar interactions within the framework of a modified SPM behavior [40], giving a first indication of direct support for the evolution of the relaxation time versus the interaction strength according to the Dormann model.

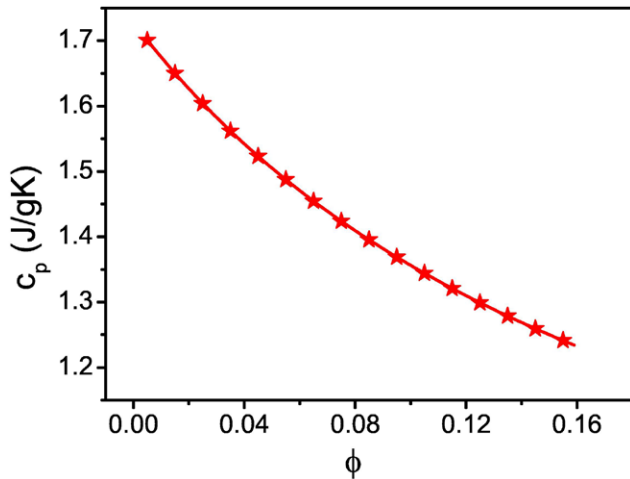


Figure 3. Specific heat capacity (c_p) dependence on the sample volume fraction (ϕ) at a temperature of 15 °C.

The temperature dependence of the dynamic viscosity ($\eta(T)$) of transformer oil was measured with a Hoppler viscosimeter in the (15–80 °C) temperature range. The temperature and volume fraction dependencies of the ferrofluid specific heat capacity ($c_p(T, \phi)$) can be obtained by the mixed extrapolation of discrete points from differential scanning calorimetry (DSC) curves (e.g. as exemplified in figure 2 for the sample with the lowest dilution) collected for samples of different volume fractions. However, due to the constant slope of the $c_p(T)$ dependence for all considered volume fractions, it was enough to provide the values of $c_p(\phi)$ at a constant temperature (e.g. at 15 °C) and then to express analytically $c_p(T)$ for each volume fraction. Accordingly, figure 3 shows the variation of c_p with ϕ at 15 °C.

Furthermore, the variation of the specific heat capacity versus temperature at a specified volume fraction is given by:

$$c_p(T, \phi) = (c_p(\phi))_{T_i=15\text{ }^\circ\text{C}} + 0.0023 \times T(^\circ\text{C}). \quad (5)$$

3. Results and discussions

In order to quantitatively analyze the effects of the interparticle interactions on SAR in ferrofluids excited by AC magnetic fields, the heating profile of different samples ($T(t)$) has been recorded. For taking into account the heat losses, unavoidable in this kind of calorimetric experiment, a recently developed methodology [39] has been applied. It is worth mentioning that an alternative way of diminishing the effect of heat losses (faster, but less efficient) is by taking the initial slope of the recorded heating curve [43, 44].

According to the developed methodology, a typical heating–cooling cycle $T_H(t) \rightarrow T_C(t)$ for the sample with the lowest volume fraction, $\phi_1 = 0.005$, subjected to $H_{01} = 14 \text{ kA m}^{-2}$ is shown in the inset of figure 4. Both heating ($T_H(t)$) and cooling ($T_C(t)$) curves were fitted with appropriate functions and following the procedure described in [39], the adiabatic-like heating curve was finally generated (figure 4—red empty circles). This methodology was applied for all recorded heating–cooling cycles (corresponding to the analyzed samples of

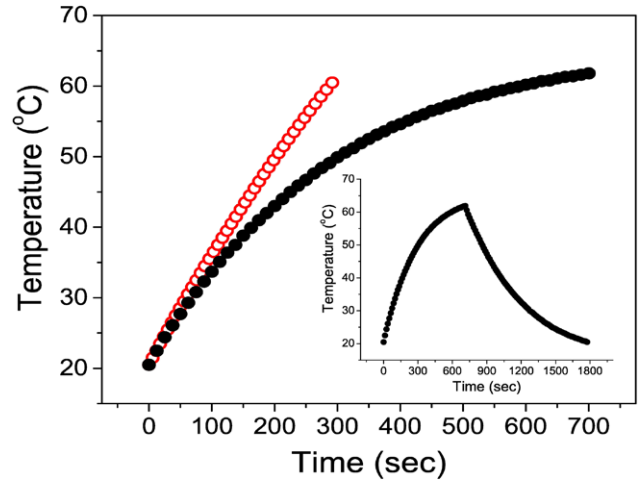


Figure 4. The adiabatic-like and real heating curves (red empty and black full circles, respectively) for the sample with $\phi_1 = 0.005$ and excited under a field amplitude $H_{01} = 14 \text{ kA m}^{-1}$. The heating–cooling cycle is shown in the inset of the figure.

different volume fractions and excited by different field amplitudes).

A pure superparamagnetic regime can be assumed without a doubt for the sample with the lowest dilution due to its low volume fraction $\phi_1 = 0.005$. The adiabatic heating curve $T(t)$ can be theoretically simulated in this case by using the model by Rosensweig [30], which is valid only for magnetic nanoparticle ensembles with no mutual interactions. Accordingly, the dissipated power is $P = \mu_0 \pi f H_0^2 \chi_0 \times 2\pi f \tau / (1 + (2\pi f \tau)^2)$ where τ is the effective relaxation time related to both Brownian and Neel relaxation mechanisms accounted by the specific temperature-dependent relaxation times τ_B and τ_N , ($1/\tau = 1/\tau_B + 1/\tau_N$), f and H_0 are the frequency and the amplitude of the applied AC magnetic field, μ_0 is the air permeability and χ_0 is the equilibrium susceptibility. For the present systems, the Neel relaxation mechanism is strongly dominant (average particle radius lower than 6 nm). The equilibrium susceptibility may be approximated by the initial susceptibility, χ_i , expressed via $\chi_i = \mu_0 \eta M_D^2 V_M / 3k_B T$ with M_D and V_M the spontaneous magnetization and the magnetic volume of the nanoparticle, respectively. Taking into account the physical parameters of the ferrofluid sample, the corresponding anisotropy energy ($(KV)_1 = 0.62 \times 10^{-20} \text{ J}$) and temperature variations of c_p and η , the theoretical heating curve leads to the best fit of the experimentally obtained adiabatic-like curve for $\tau_0 = 4.5 \times 10^{-9} \text{ s}$ (figure 5). It is worth mentioning here that for none of the analyzed samples further presented was possible to obtain a convenient fit over the whole time/temperature range. An accurate justification of this fit deficiency observed as the volume fraction increases is found to be nontrivial. Therefore, taking into account that the most appropriate thermal equilibrium states are obtained in the first heating stages where the thermal losses can also be neglected, the fit of the theoretical to the experimental heating curve has been adjusted mainly with respect to the initial slope (as will be shown in the following such fit extended over a lower temperature range for samples of increasing volume fraction).

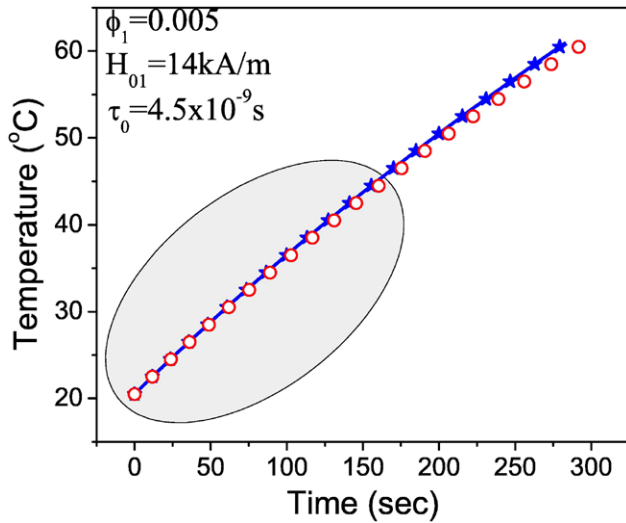


Figure 5. Experimental adiabatic curve fitted by theoretic adiabatic curve (the range of suitable fit is marked in gray).

The next ferrofluid samples have volume fractions much higher than the first ($\phi_2 = 0.023$, $\phi_3 = 0.094$, $\phi_4 = 0.16$), which expectedly should have a certain influence on the SPM behavior of the suspended nanoparticles (modified superparamagnetism). Any attempt to fit the adiabatic-like heating curves obtained from the experimental data by keeping in the Rosensweig model the same value of τ_0 , (4.5×10^{-9} s) and considering in equation (2) of the relaxation time (for an assumed modified SPM) the corresponding values for the anisotropy energies as derived from figure 1, was not successful (see, for example, the insets of figures 6 and 7). Differences between the initial slopes of these curves (theoretical and adiabatic-like) are always present and increase with the volume fractions). In order to improve the accuracy of the fit (with focus on the initial slope) the presence of the ‘glass-like’ behavior was also tested by using relation (3) for the Neel expression of the relaxation time. Implausible values for T_0 improving the fit were obtained. Therefore, the only solution to reach a good fit, at least over the initial slopes, was to modify the values of τ_0 . In the case of the sample with the volume fraction $\phi_2 = 0.023$ and $KV_2 = 0.64 \times 10^{-20}$ J a value for τ_0 of 4.2×10^{-9} s leads to a theoretical heating curve, whose initial slope coincides with that of the experimentally obtained adiabatic-like ($v_{A_{th}(i)} = v_{A_{exp}(i)}$). For the ferrofluid sample with volume fraction ϕ_3 and anisotropy energy barrier $KV_3 = 0.72 \times 10^{-20}$ J the difference between the experimental and theoretical adiabatic initial slopes increases by about twice ($v_{A_{exp}(i)} = 0.018 \text{ }^\circ\text{C s}^{-1}$ and $v_{A_{th}(i)} = 0.038 \text{ }^\circ\text{C s}^{-1}$) if τ_0 is maintained in the theoretical model at the initial value corresponding to non-interacting NPs (see the inset of figure 6). The best fit of the initial experimental slope (see the gray area in figure 6) is obtained for $\tau_0 = 2.1 \times 10^{-9}$ s in the theoretical heating curve.

In the case of the sample with the highest volume fraction ϕ_4 used in this experiment, the theoretical initial slope is 2.5 times greater than the experimental adiabatic one ($v_{A_{exp}(i)} = 0.010 \text{ }^\circ\text{C s}^{-1}$ and $v_{A_{th}(i)} = 0.027 \text{ }^\circ\text{C s}^{-1}$) for the initial value of τ_0 and $KV_4 = 0.78 \times 10^{-20}$ J. The best fit of the

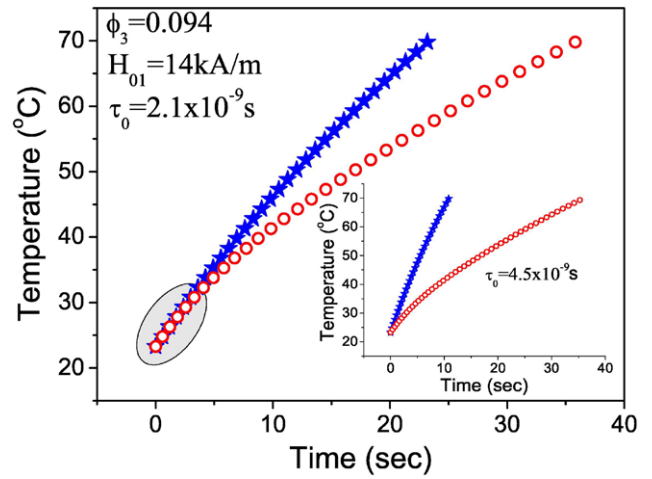


Figure 6. Experimental adiabatic curve fitted by theoretic adiabatic curve for $\tau_0 = 2.1 \times 10^{-9}$ s. Inset of the figure shows the fit for $\tau_0 = 4.5 \times 10^{-9}$ s.

experimental curve over the largest temperature interval (as presented in figure 7 in the gray zone) was found by taking $\tau_0 = 1.75 \times 10^{-9}$ s. It is noted that the restricted range of the reasonable fit of the adiabatic-like curves is derived from the experimental data in the case of the samples of high volume fraction. It is not easy to provide a precise answer to this shortcoming, due to the different potential origins of either the methodological or phenomenological type as, for example, underestimated heat losses which might be amplified at larger heating time and for higher field amplitudes, a possible dependence of the relaxation time constant versus temperature, a time-dependent thermal transfer, etc.

The evolution of the obtained values of τ_0 (leading to the best fit of the slope in the adiabatic-like heating curve derived from the experimental data) versus the volume fraction, shows an exponential-like decrease behavior (figure 8). It is noted that a similar evolution of τ_0 was evidenced for all four magnetic field intensities used in the experiments (inset of figure 8)

According to Rosensweig’s model, the dissipated volumetric power is directly proportional to the volume fractions. However, as shown above, the dipolar interactions between the nanoparticles inhibit the superparamagnetic relaxation of the system by decreasing the constant time τ_0 corresponding to the modified SPM given by equation (2). Therefore, it is worth quantifying the influence of the dipolar interactions on the SAR, which in the case of a ferrofluid with volume fraction ϕ , can be expressed by:

$$\text{SAR}(T) = q_p(T)/m = c(T, \phi)v_A(T) \quad (6)$$

where $q_p(T)$ is the volumetric power dependent on the temperature, m is the mass of the ferrofluid sample, $c(T, \phi)$ – is the specific heat capacity of the sample and $v_A(T) = (dT/dt)_T$ is the heating speed evaluated under adiabatic-like conditions. In order to measure the volume fraction dependence of the SAR, the initial heating speeds of the experimental adiabatic curves for all samples subjected to all four magnetic field intensities were considered. The associated SAR values were compared to the SAR values generated by the theoretical

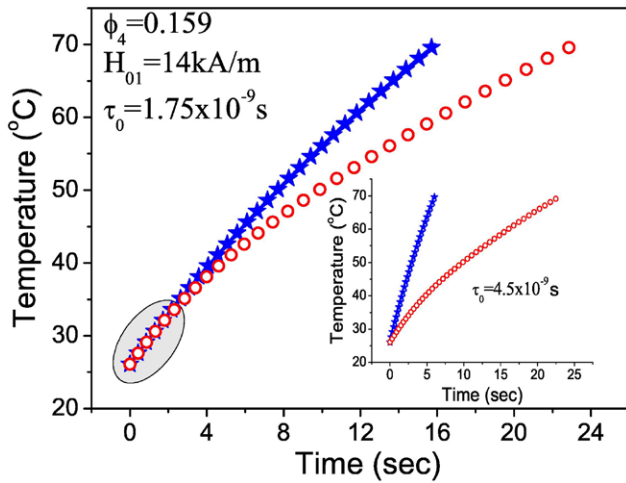


Figure 7. Experimental adiabatic curve fitted by theoretic adiabatic curve for $\tau_0 = 1.75 \times 10^{-9}$ s. Inset of the figure shows the fit for $\tau_0 = 4.5 \times 10^{-9}$ s.

model, without taking into account any influence of the interaction (e.g. the change of the anisotropy energy barrier and of parameter τ_0). These comparisons are shown in figure 9 (for $H_{01} = 14 \text{ kA m}^{-1}$, $H_{02} = 21 \text{ kA m}^{-1}$, $H_{03} = 28 \text{ kA m}^{-1}$ and $H_{04} = 35 \text{ kA m}^{-1}$). For equivalent non-interacting particulate systems corresponding to all samples, the anisotropy energy barrier was kept constant and equal to that of the lowest volume fraction $(KV)_1 = 0.62 \times 10^{-20} \text{ J}$ and τ_0 was kept at the same value of 4.5×10^{-9} s characteristic of the pure superparamagnetic regime.

In respect to the theoretical model [30], the power dissipated (or SAR) by a pure SPM system (without interparticle interactions) excited with AC magnetic fields grows almost linearly with the volume fraction. However, according to figure 9, the experimental SAR values corresponding to real systems of interacting nanoparticles, presents a much weaker increase. The relative diminution of the experimental SAR values with respect to the theoretical values estimated in the case of non-interacting NPs becomes more pronounced with both the volume fraction and amplitude of the exciting AC magnetic field (see figures 9(a)–(d)). Therefore, the dipolar interactions between the nanoparticles in the modified SPM regime introduce a dramatic negative influence on SAR, reducing implicitly the hyperthermic potential of the system.

Concerning the explanation of the observed reduced transferred power in the presence of inter-particle interactions, it is worth mentioning that starting from the above-mentioned dependence of the dissipated power and using relation (1) with the actually derived values of τ_0 and KV , it results in a dependence of type $P \sim \tau$. Furthermore, by taking for τ_0 and KV specific values for systems without interparticle interactions (e.g. for volume fraction ϕ_1) and, respectively, with interparticle interactions (e.g. for volume fraction ϕ_3), the resulting relaxation time given by equation (1) is lower in the presence of dipolar interactions. A reduced transferred power is also expected in this case.

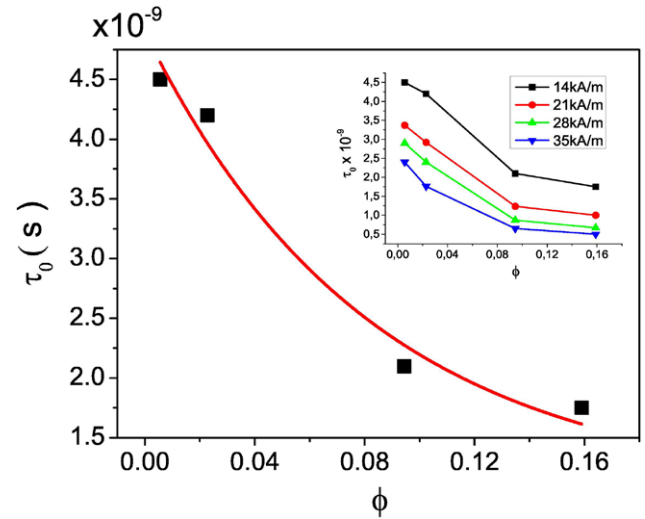


Figure 8. Evolution of SPM time constant (τ_0) in seconds, in respect of the volume fraction. Inset of the figure shows the same evolution corresponding to different magnetic field intensities (the lines are only for a visual guide).

A reduced specific absorption rate on the unit mass of the magnetic component was reported in [11] as the effect of inter-particle interactions. Expectedly, the SAR values reported in [11] should remain constant, whereas the SAR values reported in this work (relative to the unit mass of ferrofluid) should increase linearly with the volume fraction, if no intrinsic effects of the inter-particle interactions are present. In fact, the negative deviation from the linear increase of the SAR values versus the volume fraction, as observed in this work (see figure 9), is in agreement with the decreased SAR behavior at increasing volume fractions (compared to the expected constant one) reported in [11], showing a similar effect of inter-particle interactions on the specific absorption rate.

It is worth noting that the experimentally derived dependence of both the anisotropy energy barrier and relaxation time constant versus the volume fraction has direct implications for the theoretical modeling of MFH, which is required for the estimation of the heat transfer term to be used as the input parameter for the numerical solutions of the bio-heat transfer equation.

4. Conclusions

The effect of magnetic interparticle interactions in SPM systems on the magnetic relaxation process is of particular importance in the magnetic hyperthermia procedure. This effect was carefully investigated in terms of a modified SPM state, using experimental evaluations on ferrofluid samples based on coated magnetite nanoparticles, with volume fractions ranging from very low values (approaching the pure SPM regime of NPs) to medium values (modified SPM regime of NPs). The influence of the modified SPM behavior on the specific absorption rate of the ferrofluid samples was investigated by calorimetric measurements, taking into account the modification of the magnetic anisotropy energy barrier in respect of the volume

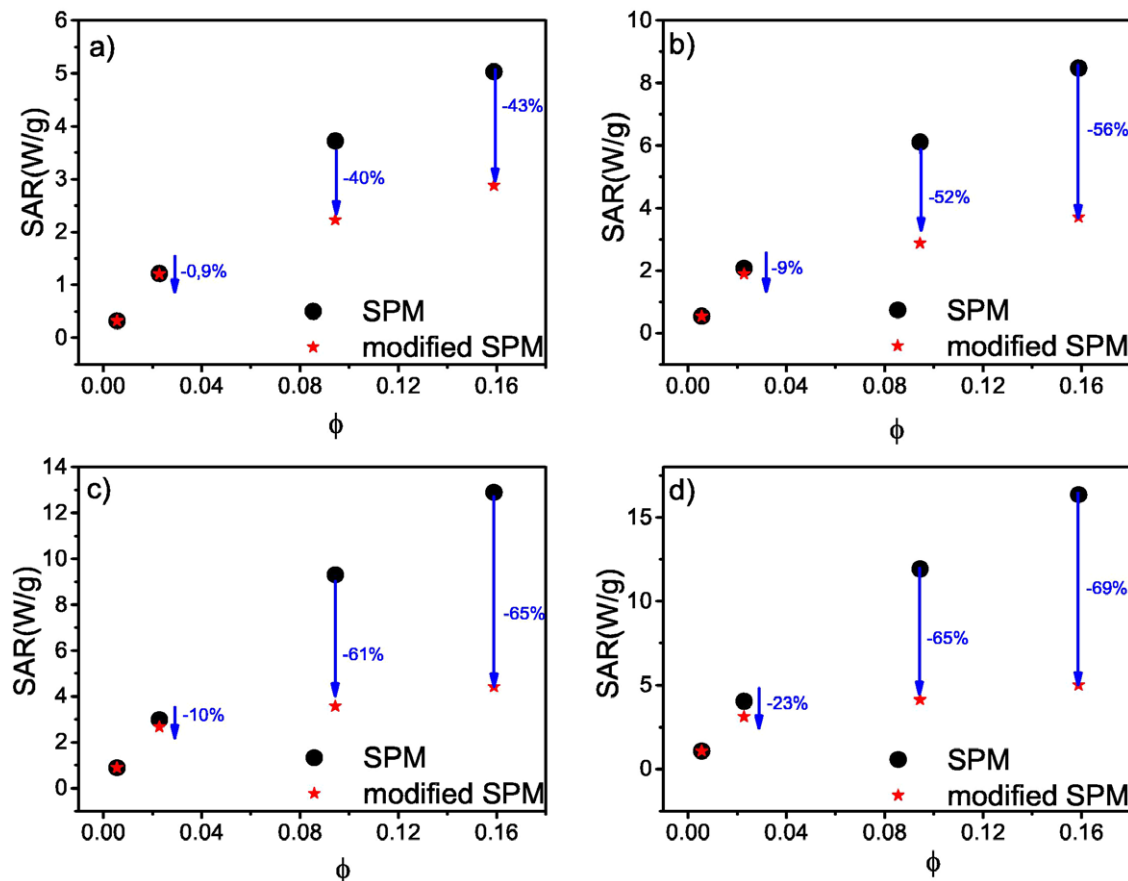


Figure 9. Specific absorption rate versus the volume fraction in the case of non-interacting (full circles) and interacting (stars) superparamagnetic nanoparticles at different amplitudes of the AC magnetic field: 14 kA m^{-1} (a), 21 kA m^{-1} (b), 28 kA m^{-1} (c), 35 kA m^{-1} (d).

fraction evidenced by the specific magnetic measurements. It was found that the presence of the magnetic dipolar interactions among the NPs leading to the modified SPM regime also influences the time constant (τ_0) in the Neel–Brown relaxation law, with this quantity becoming a system-dependent constant, changing with both NP characteristics and concentration. As a direct consequence of the diminished relaxation process in the modified SPM, the increased SAR versus the volume fraction (of crucial importance in modeling bio-transfer equations for the simulation of the temperature distribution in the tissue) is much lower than in the case of non-interacting similar NPs.

Acknowledgments

The financial support, through the exploratory research projects PCE IDEI 75/2011 and Core Program PN16-480103, is gratefully acknowledged by the authors from NIMP. N Iacob was supported by the strategic grant POSDRU/159/1.5/S/137750, ‘Project Doctoral and Postdoctoral programs support for increased competitiveness in Exact Sciences research’, co-financed by the European Social Fund within the Sectorial Operational Program Human Resources Development 2007–2013. The FF samples investigated in this work were prepared by SC ROSEAL SA, Odorheiu Secuiesc (Romania) within the framework of the project MagNanoMicroseal, contract 157/2012, according to an original procedure developed

by Dr D Bica. The present research work was also inspired by the COST Action RADIOMAG (TD 1402).

References

- [1] Nissim A *et al* 2012 *PLoS One* **7** e40134
- [2] Teresa A P and Rocha S 2014 *TRAC Trends Anal. Chem.* **62** 28
- [3] Kenouche S *et al* 2014 *Powder Technol.* **255** 60
- [4] Ayala V *et al* 2013 *J. Nanopart. Res.* **15** 1874
- [5] Babincov M *et al* 2008 *IEEE Trans. NanoBiosci.* **7** 15
- [6] Arthur R M *et al* 2005 *Int. J. Hyperth.* **21** 589
- [7] Basel M T, Balivada S and Wang H 2012 *Int. J. Nanomed.* **7** 297
- [8] Huang H S and Hainfeld J F 2013 *Int. J. Nanomed.* **8** 2521
- [9] Blanco-Mantecon M and O’Grady K 2006 *J. Magn. Magn. Mater.* **296** 124
- [10] Branquinho L C *et al* 2013 *Sci. Rep.* **3** 2887
- [11] De la Presa P *et al* 2015 *J. Phys. Chem. C* **119** 11022
- [12] Nadeem K *et al* 2011 *J. Magn. Magn. Mater.* **323** 1998
- [13] De Toro J A *et al* 2013 *J. Phys. Chem. C* **117** 10213
- [14] Belokon V I *et al* 2013 *Adv. Mater. Res.* **774–6** 523
- [15] Guéron S *et al* 1999 *Phys. Rev. Lett.* **83** 4148
- [16] Weizenmann A, Santos M and Figueiredo W 2012 *Phys. Lett. A* **376** 1535
- [17] Neel L 1949 *Ann. Geophys.* **5** 99
- [18] Brown W F 1963 *Phys. Rev.* **130** 1677
- [19] Dormann J L, Fiorani D and Tronc E 1997 *Adv. Chem. Phys.* **98** 283
- [20] Bedanta S and Kleemann W 2009 *J. Phys. D: Appl. Phys.* **42** 013001

- [21] Petracic O 2010 *Superlattices Microstruct.* **47** 569
- [22] Tombacz E et al 2015 *Biochem. Biophys. Res. Commun.* **468** 442
- [23] Mørup S and Tronc E 1994 *Phys. Rev. Lett.* **72** 3278
- [24] Hansen M F and Mørup S 1997 *J. Magn. Magn. Mater.* **184** 262
- [25] Périgo E A et al 2015 *Appl. Phys. Rev.* **2** 041302
- [26] Miao Y et al 2012 *Int. J. Mol. Sci.* **13** 5554
- [27] Covaliu C I et al 2011 *J. Nanopart. Res.* **13** 6169
- [28] Kossatz S et al 2015 *Breast Cancer Res.* **17** 66
- [29] Ortega D and Pankhurst Q A 2013 *Nanostructures Through Chemistry* (Cambridge: Royal Society of Chemistry) p 60
- [30] Rosensweig R E 2002 *J. Magn. Magn. Mater.* **252** 370
- [31] Etheridge M et al 2014 *Technology* **2** 214
- [32] Coral D F et al 2016 *Langmuir* **32** 1201
- [33] Jeun M et al 2009 *Appl. Phys. Lett.* **95** 082501
- [34] Elsherbini A M and El-Shahawy A 2013 *J. Nanomater.* **2013** 467878
- [35] Mehdaoui B et al 2013 *Phys. Rev. B* **87** 174419
- [36] Haase C and Nowak U 2012 *Phys. Rev. B* **85** 045435
- [37] Patel R, Sookoor J, Bud'ko L, Ewing S and Zhang E C 2014 *Mater. Sci. Eng. C* **42** 52
- [38] Conde-Leboran I et al 2015 *J. Phys. Chem. C* **119** 15698
- [39] Iacob N, Schinteie G, Palade P and Kuncser V 2015 *J. Nanopart. Res.* **17** 190
- [40] Schinteie G, Palade P, Vekas L, Iacob N, Bartha C and Kuncser V 2013 *J. Phys. D: Appl. Phys.* **46** 395501
- [41] Iacob N, Schinteie G, Palade P, Ticos C M and Kuncser V 2015 *Eur. Phys. J. E* **38** 57
- [42] Bica D 1995 *Rom. Rep. Phys.* **47** 265
- [43] Bekovic M and Hamler A 2010 *IEEE Trans. Magn.* **46** 552
- [44] Zhao Q et al 2012 *Theranostics* **2** 113